Development 124, 3197-3207 (1997)
Printed in Great Britain © The Company of Biologists Limited 1997
DEV5142



# *mago nashi* mediates the posterior follicle cell-to-oocyte signal to organize axis formation in *Drosophila*

**Phillip A. Newmark†, Stephanie E. Mohr, Lei Gong and Robert E. Boswell***

Howard Hughes Medical Institute, Department of Molecular, Cellular, and Developmental Biology, University of Colorado, Boulder, Colorado 80309-0347, USA

*Author for correspondence (e-mail: boswell@spot.colorado.edu)
†Current address: Department of Embryology, Carnegie Institution of Washington, 115 W. University Parkway, Baltimore, MD 21210, USA

## SUMMARY

**Establishment of the anteroposterior and dorsoventral axes in the *Drosophila* egg chamber requires reciprocal signaling between the germ line and soma. Upon activation of the *Drosophila* EGF receptor in the posterior follicle cells, these cells signal back to the oocyte, resulting in a reorganization of the oocyte cytoplasm and anterodorsal migration of the oocyte nucleus. We demonstrate that the gene *mago nashi* (*mago*) encodes an evolutionarily conserved protein that must be localized within the posterior pole plasm for germ-plasm assembly and *Caenorhabditis elegans mago* is a functional homologue of *Drosophila mago*. In the absence of *mago*$^+$ function during oogenesis, the anteroposterior and dorsoventral coordinates of the oocyte are not specified and the germ plasm fails to assemble.**

Key words: *Drosophila*, axis formation, germ plasm, *mago nashi*, follicle, oocyte, signaling

## INTRODUCTION

Formation of the anteroposterior and dorsoventral axes of *Drosophila* requires inductive interactions between the germ-line-derived oocyte and surrounding somatic follicle cells during oogenesis (Ray and Schüpbach, 1996). These inductive interactions require *gurken* (*grk*) function in the germ line and *torpedo* (*top*) function in the somatic follicle cells (González-Reyes et al., 1995; Roth et al., 1995). During early oogenesis, when the germinal vesicle is located at the posterior end of the developing egg chamber, Grk protein (a member of the transforming growth factor α family) is necessary to induce the localized activation of the *top*-encoded *Drosophila* epidermal growth factor receptor (top/DER) in a subset of posterior follicle cells (González-Reyes et al., 1995; Roth et al., 1995). Grk-induced activation of the top/DER tyrosine kinase is likely to lead to Ras signaling in these follicles, causing them to adopt a posterior fate. It has been proposed that these posterior follicle cells in turn send a signal back to the oocyte. Neither the ligand produced by the posterior follicle cells nor the receptor on the oocyte have been identified, but it appears that protein kinase A is necessary in the oocyte for the signal to be transduced (Lane and Kalderon, 1994). Reception of the posterior follicle cell signal by the oocyte induces a reorganization of the oocyte microtubule cytoskeleton (stages 6-7), movement of the oocyte nucleus to an anterodorsal position (stage 8), and localization of germ cell and abdominal determinants within the posterior pole plasm (stages 8-14) (González-Reyes et al., 1995; Roth et al., 1995). This reorganization of cytoplasmic determinants leads to cellular differentiation during embryogenesis.

To study the localization and function of these determinants, maternal effect mutations that impair the formation and function of the posterior pole plasm (germ plasm) have been isolated. Females carrying mutations in the posterior group genes, *cappuccino*, *mago nashi*, *oskar*, *spire*, *staufen*, *tudor*, *valois* and *vasa*, produce embryos with defects in abdominal segmentation and germ cell formation (Boswell and Mahowald, 1985; Lehmann and Nüsslein-Volhard, 1986; Schüpbach and Wieschaus, 1986; Manseau and Schüpbach, 1989; Boswell et al., 1991). In each of these cases, polar granules (germ-plasm-specific organelles) fail to assemble during oogenesis and the progeny of mutant females lack germ cells.

Detailed analysis of the posterior group genes reveals that the posterior pole plasm is assembled in a step-wise manner, with earlier acting components required for the localization of later components (for review, see St. Johnston, 1993). For example, mislocalization of *oskar* (*osk*) mRNA to the anterior pole of the oocyte is sufficient to direct the assembly of a functional ectopic posterior pole plasm (Ephrussi and Lehmann, 1992). This leads to the formation of polar granules at the anterior pole, anterior recruitment of Vasa and Tudor proteins, anterior localization of the abdominal segmentation determinant (*nanos* mRNA; Wang and Lehmann, 1991), and induction of ectopic germ cell formation and abdominal segmentation (Ephrussi and Lehmann, 1992; Bardsley et al., 1993). Females carrying the *osk* mislocalization construct and mutations in the genes *cappuccino*, *mago nashi*, *spire* or *staufen* assemble functional germ plasm at the anterior pole (Ephrussi and Lehmann, 1992). Based on these studies, it appears that the *cappuccino*,

*mago nashi*, *spire*, and *staufen* gene products play a role in the posterior localization of *osk* mRNA. Once localized, *osk* mRNA directs the assembly of the germ-plasm components and the localization of the abdominal segmentation determinant *nanos*.

As with most posterior group genes, the sequence of *mago nashi* (*mago*) does not immediately suggest a biochemical role for the protein (Newmark and Boswell, 1994). To help clarify the role of *mago* in development, we have extended the phenotypic analysis of *mago* mutants and isolated homologues of *Drosophila mago*. Our extended phenotypic characterization demonstrates that, by mediating the response of the oocyte to the *grk-top/DER*-induced signal transmitted by the posterior follicle cells, *mago*$^{+}$ is involved in the establishment of antero-posterior and dorsoventral polarity as well as assembly of a functional posterior pole plasm. We also show that Mago protein is transiently localized within the posterior pole during two distinct stages of oogenesis. This posterior pole localization is dependent on the wild-type functions of *cappuccino*, *spire* and *grk*. In addition, we have identified homologues of *Drosophila mago* in *Caenorhabditis elegans*, *Xenopus laevis* and *Mus musculus*. We demonstrate that the most distantly related gene, *C. elegans mago*, is a functional homologue of *Drosophila mago*, suggesting that components of germ-plasm assembly have been conserved over large evolutionary time frames.

## MATERIALS AND METHODS

### Fly stocks and culturing

The *mago* alleles used in this work (*mago*$^{1}$, *mago*$^{3}$, *WE7*, *RE7* and *SHL-1*), the deletion *Df(2R)F36*, as well as the mutations *capu*$^{G7}$, *spir*$^{RP48}$, *vas*$^{PD}$ and *grk*$^{HK}$ were maintained in stocks containing *Df(1)w, y w*$^{67c23}$ X chromosome(s) and an *In(2LR)SM5* (*SM5*) balancer chromosome (Lindsley and Zimm, 1992). Flies were cultured in half-pint milk bottles or in 8-dram vials on standard *Drosophila* medium.

Eggs were collected for egg counts and observation of egg shells on 60×15 mm plates containing apple juice agar medium (Wieschaus and Nüsslein-Volhard, 1986). Females were reared at 25˚C, eggs were collected at 12 hour intervals for 2-3 days, chorions were initially viewed with a Leica MZ6 dissecting microscope and subsequently mounted for observation using a Zeiss axiophot microscope as described by Wieschaus and Nüsslein-Volhard (1986). After rearing females for 2-3 days at 25˚C, females were shifted to 17˚C, eggs were collected at 12 hour intervals and eggs shells were observed as described above. The production of ventralized eggs increases 4 days after shifting females from 25˚C to 17˚C. Females reared continuously at 17˚C did not produce ventralized eggs but ~30-40% of stage 10 egg chambers contained an oocyte nucleus localized within the posterior pole.

Germ-line and follicle cell mosaics were produced as described by Chou and Perrimon (1996).

### Construction and characterization of transgenes encoding N-terminal-tagged Mago proteins

Synthetic oligonucleotides (Operon, Inc.) encoding a myc-epitope (*Dsa*/*myc*: 5′-CACGATGGAGCAAAAGCTTATTAGCGAGGAAGATCTGAATTC-3′ and *Dsa*/AS-*myc*: 5-CGTGGAATTCAGATCTTCCTCGCTAATAAGCTTTTGCTCCAT-3′) were annealed and cloned into a unique *Dsa*I recognition site in the *mago* cDNA, p5A (Newmark and Boswell, 1994), resulting in pMyc5A. An *Mlu*I-*Stu*I fragment derived from pMyc5A was used to replace the corresponding fragment of the *mago* transformation vector pCaS4-B/P2.2 (Newmark and Boswell, 1994). DNA sequencing was performed to confirm the incorporation of *myc*-encoding sequences into *mago* genomic DNA and the resulting construct, pCaS4-*myc-mago*, was co-injected into *w*$^{1118}$ embryos with pπ25.7wc helper plasmid. One X-linked homozygous viable insertion was obtained, p[*myc-mago*].

The p[*myc-mago*] element on the X chromosome was mobilized using Δ2-3 as a genomic source of transposase activity (Robertson et al., 1988). Fourteen independent autosomal insertions were examined for the production of myc-Mago by immunoblot analysis using affinity-purified, anti-Mago antibodies (see below) and whole-mount immunofluorescence (see below).

The *mago*$^{1}$ mutation (GLY 19→ARG; Newmark and Boswell, 1994) was introduced into the corresponding codon in pMyc5A using the oligo 5′-GAATTCGTGCCTGAACTTGCCC-3′ with the Sculptor in vitro mutagenesis kit (Amersham). Introduction of the mutation was confirmed by DNA sequencing and the construct was subcloned into pCaS4-B/P2.2 as described for pCaS4-*myc mago*, resulting in pCaS4-*myc-mago*$^{1}$. A single second chromosome-linked insertion, p[*myc-mago*$^{1}$], was recombined onto a chromosome with the zygotic lethal *mago* allele *SHL-1* and the distribution of myc-Mago$^{1}$ was determined in ovaries from homozygous p[*myc-mago*$^{1}$] *SHL-1* females (see below).

GFP-tagged *mago* was constructed by inserting blunt-ended GFP sequence into the unique *Dsa*I restriction site in p5A, replacing the *Mlu*I-*Xba*I fragment of pCaS4-B/P2.2 with the corresponding fragment of pGFP5A and sequencing to confirm the in-frame incorporation of GFP into the *mago* gene. One X-linked, viable insertion, p[*GFP-mago*], was obtained by P-element-mediated transformation.

The distribution of GFP-Mago protein in p[*GFP-mago*]; *Df(2R)F36/CyO* females was determined by dissecting ovaries in PBST (1× PBS, 0.1% Triton X-100) and fixing for 15 minutes in 4% paraformaldehyde, PBST. Samples were examined by epifluorescence microscopy using a Zeiss axiophot and analyzed using a Molecular Dynamics MultiProbe 2001 confocal microscope.

### Construction of Mago fusion proteins for antibody production and purification

To construct a maltose-binding protein (MBP)-Mago fusion protein, a *mago* cDNA fragment was cloned into pMAL-c2 (New England Biolabs). This construction (pMal-5A) was confirmed by DNA sequencing and results in an MBP-Mago fusion protein (Mago at C terminus) of $59\times10^{3}$ $M_{r}$ upon induction with IPTG. Large-scale purification of the soluble MBP-Mago fusion protein was performed by affinity chromatography on an amylose resin following the recommendations of the supplier (NEB). Purified MBP-Mago was then dialyzed against multiple changes of PBS and injected into three rats at a concentration of ~400 μg/mL. Commercial injections and bleeds were performed at the Pocono Rabbit Farm and Laboratories (Canadensis, PA).

### Affinity purification of anti-Mago antibodies using 6×His-Mago fusion protein

Antisera obtained from the rats immunized with the MBP-Mago fusion protein recognize an approximately $17\times10^{3}$ $M_{r}$ protein in *Drosophila* ovarian extracts. Anti-Mago antibodies were affinity purified using a 6×His-Mago fusion protein. The 6×His-Mago fusion protein was generated by in-frame insertion of *mago* cDNA sequence into pQE-8 (Qiagen), resulting in pQE-*mago*. Insoluble 6×His-Mago protein was purified under denaturing conditions by metal chelate affinity chromatography on Ni-NTA resin as recommended by the supplier (Qiagen). Eluted 6×His-Mago protein was dialyzed into PBS/0.1% SDS and coupled to AminoLink gel following the recommendations of the supplier (Pierce). Rat anti-sera were diluted 1:10 in PBS and circulated over a column containing the soluble protein fraction from IPTG-induced *E. coli* cells containing the pMAL-c2 vector alone. The flow-through from this column was then circulated

over the 6×His-Mago affinity column, washed and eluted with 0.1 M glycine (pH 2.8) into 1/10 volume of 1 M Tris-Cl (pH 8.0). Protein-containing fractions were pooled, BSA was added to 1 mg/ml and fractions were dialyzed into PBS/0.02% Na-azide. The specificity of affinity-purified material was examined by immunoblot analysis on total protein isolated from *Drosophila* ovaries.

### Immunoblot analysis

Total protein isolated from *Drosophila* ovaries was separated on tricine-SDS-polyacrylamide gels (Shägger and von Jagow, 1987). 10% T, 3% C gels were used for most applications. Ovaries were frozen on dry ice and homogenized in 1× sample buffer (4% SDS, 12% glycerol, 50 mM Tris-Cl (pH 6.8), 2% mercaptoethanol, 0.01% brilliant blue G), refrozen, thawed, passed through a 22-gauge needle and then boiled for 5 minutes prior to gel loading. After electrophoresis, gels were electro-transferred to nitrocellulose (0.2 μm pore size) in a Hoefer SemiPhor semidry blotting apparatus. Primary antibodies were diluted in Blotto/Tween (PBS or TBS, 5% non-fat dry milk, 0.1% Tween-20) and incubated overnight at 4°C. 9E10 monoclonal antibody (courtesy of Robert Cary and Michael Klymkowsky) was used at 2 μg/mL and α-Mago antibodies were used at 1:250. HRP-conjugated α-rat IgG secondary antibody (Pierce) was used at 1:25,000 and HRP-conjugated α-mouse IgG (Amersham) was used at 1:1000. Blots were washed and processed for detection using enhanced chemiluminescent (ECL) reagents as recommended by the supplier (Amersham).

### Whole-mount immunodetection and in situ hybridization on ovarian tissue

Ovaries were dissected in 1× EBR (130 mM NaCl; 10 mM Hepes (pH 6.9); 5 mM KCl; 2 mM $CaCl_2$) or PBST from females fed on wet yeast paste for 2-4 days after eclosion. For detection of myc-tagged proteins, fixation was as described by Peifer et al. (1993) or Xue and Cooley (1993). Similar results were obtained using either fixation protocol. α-myc monoclonal antibody 9E10 was used at 2-4 μg/mL (in PBSTB). Secondary antibodies were used in these concentrations: goat α-mouse-FITC or goat α-mouse-Texas Red (Amersham), 1:100; horse α-mouse-FITC (Vector), 1:250. Samples were examined by epifluorescence microscopy using a Zeiss axiophot and analyzed using a Molecular Dynamics MultiProbe 2001 confocal microscope.

Detection of Gurken protein was as described in Roth et al. (1995). Anti-Gurken antibodies (kindly provided by T. Schüpbach) were preabsorbed to ovaries from homozygous *gurken*$^{HK}$ females and used at a final dilution of 1:1000. HRP-conjugated goat α-rat secondary antibodies (Pierce) were used at a dilution of 1:100.

Localization of kinesin-βgal fusion protein (Clark et al., 1994) was determined in ovaries from *mago*$^{1}$/*Df(2R)F36*;*kinesin-LacZ*/+ and *mago*$^{1}$/SM5;*kinesin-LacZ* control females. Ovaries were fixed in 4% paraformaldehyde, PBST for 30 minutes. The fusion protein was detected by immunofluorescence staining with mouse α-βgal antibodies (Promega) at 1:500 dilution and FITC-conjugated horse α-mouse secondary antibodies (Vector) at 1:250 dilution.

In situ hybridizations were performed as described by Klingler and Gergen (1993).

### Isolation of *C. elegans mago* and construction of a *ce-mago* minigene for P-element transformation

CEESH75, a *C. elegans* expressed sequence tag with significant similarity to *Drosophila mago* (Newmark and Boswell, 1994) was provided by Anthony Kerlavage and used to screen a *C. elegans* embryonic cDNA library (Barstead and Waterston, 1989; provided by Natasha Singh and Min Han). PCR was used to determine insert sizes of the positive plaques and the clone with the largest insert (*ce-mago*2B) was sequenced. The linker used for cloning this cDNA occupies the likely position of the start codon and creates a unique *Bsp*EI site. *ce-mago*2B was digested with *Bsp*E1, filled in with Klenow, digested with *Xho*I and ligated into *Dsa*I-digested p5A (*mago* cDNA) that had been blunt-ended with Klenow and then digested with *Xho*I. This results in the in-frame insertion of *ce-mago* coding sequences directly behind the first three codons of the *mago* cDNA. An *Mlu*I-*Xho*I fragment from this clone was then cloned into pCaS4-B/P2.2, resulting in a construct in which *ce-mago* cDNA is expressed under the control of the *Drosophila mago* promoter, with the *dm-mago* 5′ and 3′ untranslated regions left intact. The *ce-mago* transformation construct was co-injected with pπ25.7wc helper plasmid into *Df(1)w, y w*$^{67c23}$ embryos. Two homozygous viable transformant strains were obtained. The strain containing an insert on the third chromosome was used for complementation analysis with balanced mutant *mago* alleles in a *Df(1)w, y w*$^{67c23}$ background.

### Isolation of *Xenopus laevis* and *Mus musculus mago* genes

The coding sequences from *dm-mago* were amplified by PCR and used to screen a *Xenopus laevis* cDNA library (kindly provided by Michael Klymkowsky). Approximately $10^6$ phage were screened by hybridization with $^{32}$P-labelled *dm-mago* sequences at 50˚C in 6× SSC; 0.5% SDS; 5× Denhardt's solution; 500 μg/mL salmon sperm DNA and washed twice at room temperature with 2× SSC; 0.1% SDS and three times at 50˚C in 0.5× SSC; 0.1% SDS (Sambrook et al., 1989). Seven positive plaques were identified; the three largest clones (as determined by PCR) were sequenced.

The *Xl-mago* coding sequences were amplified by PCR and used to screen a *Mus musculus* cDNA library (kindly provided by Barbara Knowles). Conditions for screening of approximately $10^5$ colonies were similar to those used to identify *Xl-mago*, except that hybridization was done at 65˚C and washes were done at 37˚C and 55˚C. Ten positive colonies were identified; a full-length clone was sequenced.

## RESULTS

### Aberrant dorsoventral axis formation: mislocalization of the oocyte nucleus in egg chambers of hemizygous *mago*$^{1}$ females

Approximately 1% ($n$=365) of the eggs from hemizygous *mago*$^{1}$ females (to be referred to as *mago* eggs) raised at 25˚C are ventralized. When these females are shifted from 25˚C to 17˚C, however, approximately 38% ($n$=751) of the eggs produced are ventralized, exhibiting a phenotype similar to that observed when eggs are collected from *grk* mutant females. In eggs with defective shells, expansion of ventral fates results in an elimination of the dorsal appendages (Fig. 1A,B). Although females mutant for *top*, *grk* or *cornichon* (*cni*) produce eggs exhibiting a similar ventralized phenotype (González-Reyes et al., 1995; Roth et al., 1995), eggs and embryos from these females display striking differences from those produced by hemizygous *mago*$^{1}$ mothers. Eggs from mutant *top*, *grk* or *cni* females may lack anteroposterior polarity, as exemplified by a micropyle that is formed in place of an aeropyle at the posterior pole (González-Reyes et al., 1995; Roth et al., 1995). This is in contrast to ventralized *mago* eggs which possess an aeropyle indistinguishable from that observed in wild-type eggs (Fig. 1B, right panel), suggesting that anteroposterior patterning of the egg shell is normal. Moreover, embryos derived from ventralized eggs produced by *top*, *grk* or *cni* mutant females have defects in dorsoventral patterning, whereas ventralized *mago* eggs are not fertilized due to a defective micropyle canal and, thus, do not develop (data not shown).

At stage 7 of oogenesis, the oocyte nucleus migrates from the posterior of the oocyte to an anterodorsal cortical position.

This movement is critical for suppression of ventral and establishment of dorsal follicular cell fates because it allows apical localization of *grk* mRNA and the spatially restricted synthesis of Grk protein, the likely ligand activating the *top*/*DER* signaling pathway in the overlying follicle cells (González-Reyes et al., 1995; Roth et al., 1995). Given the nuclear migration defects observed in mutants disrupting the *grk-top*/*DER* signaling pathway, we examined the position of the oocyte nucleus in *mago* egg chambers collected from females reared at 25˚C and females that had been shifted from 25˚C to 17˚C. Approximately 1% ($n$=160) of the stage 10 *mago* egg chambers from females reared at 25˚C contained an oocyte nucleus that was mislocalized, whereas 36% ($n$=216) of the stage 10 *mago* egg chambers of females shifted from 25˚C to 17˚C had germinal vesicles within the posterior pole (Fig. 1D,F). The excellent correspondence between the percentage of egg chambers with mislocalized oocyte nuclei and ventralized eggs produced by hemizygous *mago*$^1$ females suggests that the ventralized phenotype observed in *mago* eggs results from the failure of nuclear migration to the anterodorsal cortex during oogenesis. Moreover, when the germ line is homozygous for *mago*$^1$ or *mago*$^3$ (a lethal allele, GLN$^{87}$→STOP; Newmark and Boswell, 1994), egg chambers containing oocyte nuclei mislocalized within the posterior pole and eggs with ventralized shells are observed (Table 1). To determine whether *grk* mRNA and protein are synthesized and/or properly localized, we performed in situ hybridization and immunolocalization on whole-mount egg chambers collected from wild-type, hemizygous *mago*$^1$, *mago*$^1$ germ-line mosaic and *mago*$^3$ germ-line mosaic females. Regardless of the position of the oocyte nucleus in *mago* egg chambers, *grk* mRNA and protein are always detected, and accumulate in a perinuclear position between the germinal vesicle and plasma membrane (Fig. 1C-F). This suggests that the synthesis, stability and perinuclear accumulation of *grk* mRNA and protein are not dependent on wild-type *mago* function. Clearly, the failure of the oocyte nucleus to migrate anteriorly suggests a defect in anteroposterior axis formation.

### Aberrant anteroposterior axis formation: *mago* egg chambers display defects in the organization of the oocyte microtubule cytoskeleton

In the absence of *grk-top/DER* signaling during early oogenesis (stages 1-6), the fate of the posterior follicle cells is not specified and they behave as anterior follicle cells. Failure to specify posterior follicle cell fates results in an altered polarization of the oocyte microtubule network and the oocyte nucleus fails to migrate to the anterodorsal position during stage 7 of oogenesis (González-Reyes et al., 1995; Roth et al., 1995). Altered polarization of the microtubule cytoskeleton is manifested by the localization of *bicoid* (*bcd*, the anterior determinant) mRNA at both poles, and colocalization of *osk* mRNA and kinesin-β-gal to a central region within the oocyte cytoplasm (González-Reyes et al., 1995; Roth et al., 1995). Thus, in egg chambers from mutant

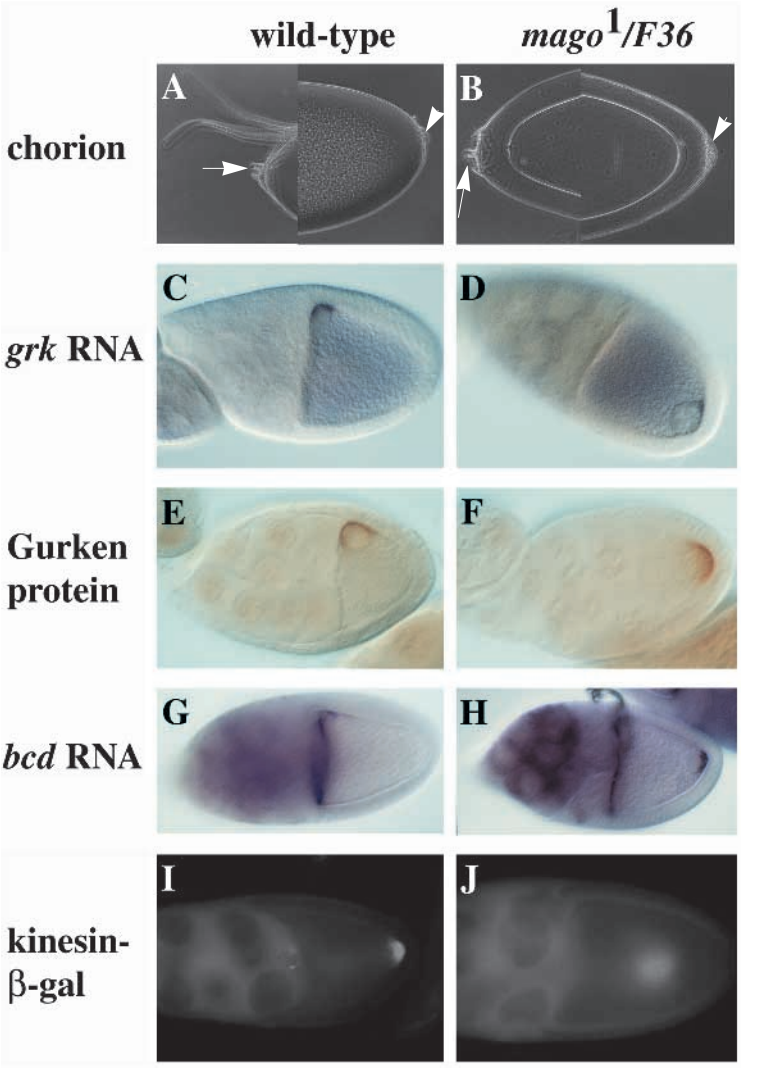


**Fig. 1**. The egg shells and egg chambers of *mago*$^1$/*Df*(*2R*)*F36* mothers exhibit defects in dorsoventral axis formation and alterations of the oocyte microtubule cytoskeleton. Eggs and egg chambers are oriented with anterior to the left and posterior to the right. Dorsal is up in A, C, E and G. (A,B) Phase-contrast micrographs of egg shells from wild-type and *mago*$^1$/*Df*(*2R*)*F36* females, respectively. The arrows indicate the position of the micropyle and arrowheads show the position of the aeropyle. In A and B, the left panel is anterior and the right panel is posterior. (A) Phase-contrast micrograph of a wild-type egg shell. The dorsal appendages and micropyle are clearly visible in the anterior. At the extreme posterior end, a rounded aeropyle is observed. (B) Approximately 38% (285/751) of the egg shells collected from *mago*$^1$/*Df*(*2R*)*F36* mothers shifted from 25˚C to 17˚C are ventralized. Dorsal appendages are not observed. However, a micropyle is visible in the anterior and an aeropyle can be seen at the extreme posterior pole. (C) Localization of the oocyte nucleus and *grk* mRNA in wild-type stage 10 egg chambers. *grk* mRNA is clearly detected between the oocyte nucleus and overlying follicle cells, indicating the position of the future dorsal surface of the egg. (D) Mislocalization of the oocyte nucleus is observed in 36% (78/216) of the stage 10 egg chambers from *mago*$^1$/*Df*(*2R*)*F36* females shifted from 25˚C to 17˚C. Perinuclear accumulation of *grk* mRNA is detected at the posterior pole with the mislocalized oocyte nucleus. *grk* mRNA accumulates between the oocyte nucleus and overlying follicle cells. (E,G,I) The distribution of Gurken protein, *bicoid* RNA and kinesin-β-gal in wild-type egg chambers, respectively. (F,H,J) The distribution of Gurken protein, *bicoid* RNA and kinesin-β-gal in egg chambers of *mago*$^1$/*Df*(*F36*) females shifted from 25˚C to 17˚C.

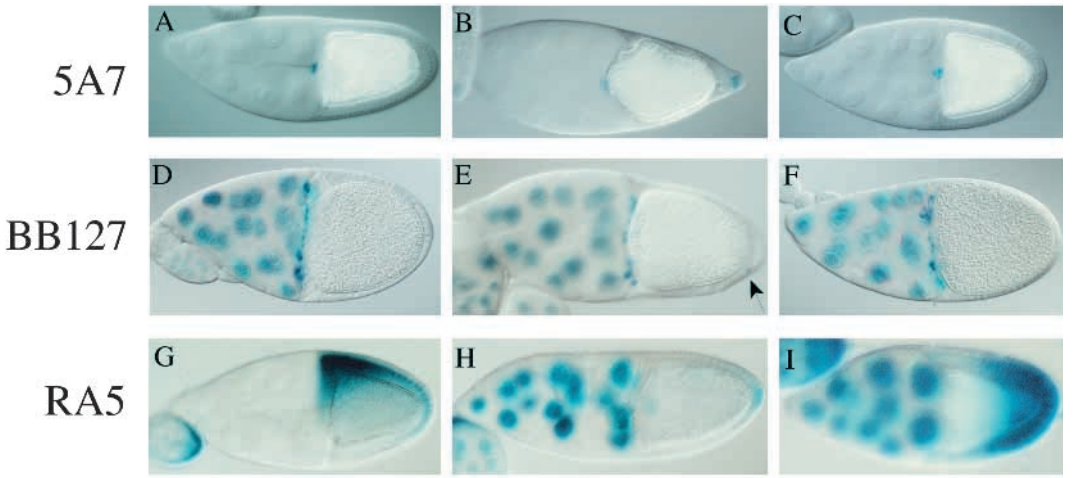


**Fig. 2**. Expression pattern of enhancer trap lines in egg chambers from wild-type and mutant females. (A-C) Females carrying the enhancer trap line p[$w^+$ *lacZ*] 5A7, which expresses β-galactosidase in the border cells. (A) Wild type; (B) homozygous $grk^{HK}$; (C) hemizygous $mago^1$ females shifted from 25˚C to 17˚. The expression pattern in *mago* egg chambers is indistinguishable from wild type. (D-F) The p[$w^+$ *lacZ*] BB127 enhancer trap line is expressed in the centripetal follicle cells and nurse cells. (D) Wild type; (E) hemizgyous $top^{QY}$; (F) hemizygous $mago^1$ females shifted from 25˚C to 17˚C. The arrow in E indicates X-gal staining in a single posterior follicle cell. In *mago* egg chambers p[$w^+$ *lacZ*], BB127 appears to be expressed in a pattern identical to wild type. (G-I) The enhancer trap line p[$ry^+$ *lacZ*] RA5 expresses β-galactosidase in the follicle cells overlying the oocyte nucleus in response to *grk* signaling. (G) Wild type; (H) homozygous $grk^{HK}$; (I) hemizygous $mago^1$ females shifted from 25˚C to 17˚C. (H,I) The females also carry the enhancer trap insertion *es*(*3*) *79* that serves to mark the nurse cell nuclei and oocyte nucleus with β-galactosidase. (C,F,I) Only *mago* egg chambers with the oocyte nucleus mislocalized within the posterior pole were counted (in each case *n*=34). In *mago* egg chambers, ectopic expression of p[$ry^+$ *lacZ*] RA5 is detected in posterior follicle cells overlying the mislocalized oocyte nucleus.

*grk*, *top* and *cni* females, both poles of the oocyte behave as anterior poles and a central region of the oocyte accumulates components normally localized within the posterior pole plasm. To ascertain whether the microtubule cytoskeleton is altered in *mago* egg chambers, we examined the distribution of *bcd* mRNA and kinesin-β-gal in *mago* egg chambers collected from females that had been shifted from 25˚C to 17˚C. In these *mago* egg chambers, *bcd* mRNA accumulates at both poles (Fig. 1G,H) and kinesin-β-gal accumulates in the center of the oocyte (Fig. 1I,J). Although *osk* mRNA and Staufen protein accumulate within *mago* egg chambers and transiently localize within the anterior pole, they do not concentrate within the posterior pole plasm or within a central ooplasmic region (Newmark and Boswell, 1994). These results indicate that polarization of the microtubule cytoskeleton is abnormal in egg chambers from hemizygous $mago^1$ females shifted from 25˚C to 17˚C, and provide further evidence that $mago^+$ function is required both for axis formation and assembly of germ-plasm components within the posterior pole.

Defects in the organization of the microtubule cytoskeleton in *mago* egg chambers may be due to the inability of Grk to signal to the overlying posterior follicle cells during oogenetic stages 1-6, or because $mago^+$ functions to mediate a signal received by the oocyte from the overlying posterior follicle cells. If *grk* signaling fails to occur in the absence of $mago^+$ function, the overlying posterior follicle cells might be expected to behave as anterior follicle cells in *mago* egg chambers (González-Reyes et al., 1995; Roth et al., 1995). Regardless of the temperature at which hemizygous $mago^1$ females are reared, enhancer-trap lines that mark anterior follicle cells are expressed in a manner indistinguishable from wild type (Fig. 2A-F). This result is consistent with the fact that the posterior aeropyle is formed normally and suggests that the fate of posterior follicle cells is specified properly. To determine whether mutations in *mago* eliminate *grk* signaling, an enhancer-trap line, RA5, that expresses β-galactosidase in response to *grk* signaling (Duffy, personal communication) was utilized. In wild-type egg chambers derived from strains containing the RA5 enhancer-trap line, β-galactosidase is detected in anterior dorsal follicle cells. However, strains containing RA5 and homozygous for mutations in *grk* produce egg chambers lacking detectable β-galactosidase in dorsal follicle cells (Fig. 2G,H, respectively). In *mago* egg chambers carrying the RA5 enhancer-trap line and in which the oocyte nucleus is mislocalized within the posterior pole, β-galactosidase is detected in posterior follicle cells overlying the germinal vesicle (Fig. 2I). The ectopic expression of β-galactosidase in the posterior follicle cells of these *mago* egg chambers indicates that $mago^1$ does not eliminate *grk* signaling. These results indicate that $mago^+$ functions within the oocyte to mediate the signal(s) sent from the posterior follicle cells to the oocyte. In the absence of wild-type *mago* function, the reorganization of the microtubule network essential for axis formation and subsequent germ-plasm assembly fails to occur.

**Table 1. Germ-line clonal analysis of *mago* alleles**

| Genotype of green line | Mislocalization of the oocyte nucleus* | Posterior pole localization of *oskar* RNA in egg chambers | Ventralized egg shells |
|---|---|---|---|
| $mago^1/mago^1$ | 4% (*n*=53) | – | 2% (*n*=701) |
| $mago^3/mago^3$ | 29% (*n*=14) | – | 19% (*n*=37) |
| $FRT^{G13}$ (control) | 0% (*n*=75) | + | 0% (*n*=699) |

Progeny from females producing $mago^1/mago^1$ germ-line clones were sterile.

*Egg chambers were reacted with antisera recognizing Gurken protein or with antisense *gurken* RNA probes. Regardless of nuclear position Gurken protein and RNA colocalize with the oocyte nucleus.

The (–) indicates no detectable localized *oskar* RNA within the posterior pole and (+) indicates localization of *oskar* RNA within the posterior pole.

### Dynamic distribution of the Mago protein during oogenesis – nuclear localization and association with the posterior pole

To examine the distribution of Mago protein in oogenesis, we first generated antibodies against Mago protein (see Materials and methods). Although these antibodies are effective for immunoblotting applications, they are less effective at detecting protein in fixed whole-mount tissues. Therefore, sequences encoding a myc-epitope (Evan et al., 1985) and the green fluorescent protein (GFP) of the jellyfish *Aequorea victoria* (Chalfie et al., 1994) were introduced into the 5′ coding sequences of the *mago* gene (see Materials and methods). Both the p[*myc-mago*] and p[*GFP-mago*] constructs were introduced into the *Drosophila* germ line using P-element-mediated transformation (Rubin and Spradling, 1982). The p[*myc-mago*] and p[*GFP-mago*] constructs complement the defects in axis formation and germ-plasm assembly of *mago*[1] and the zygotic lethality of the lethal *mago* allele, *SHL-1* (202 bp deletion of 5′ coding sequences). Immunoblot analysis using affinity-purified antibodies against Mago protein (α-Mago) was used to confirm the complementation of *SHL-1* lethality by the p[*myc-mago*] transgene (see Fig. 3). Thus, p[*myc-mago*] and p[*GFP-mago*] confer wild-type *mago* function, indicating that the N-terminal tags do not interfere with Mago protein function.

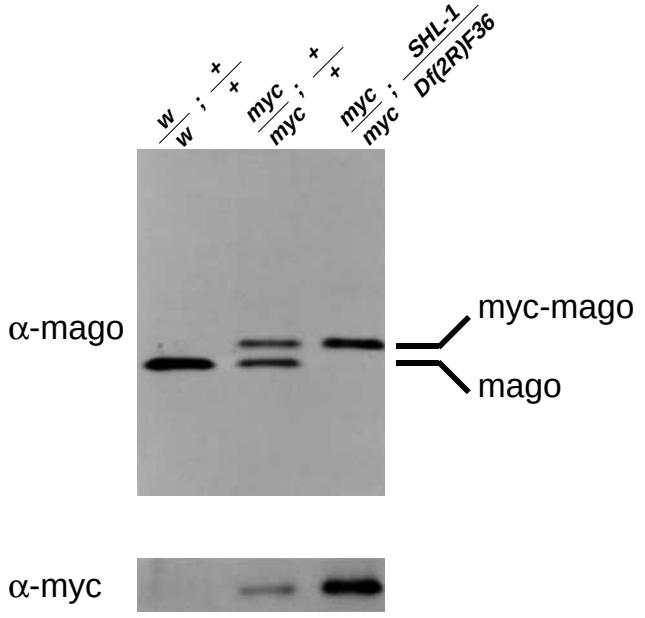


**Fig. 3**. Immunoblot analysis of Mago protein expression in ovaries. Protein extracts of ovaries from females of the indicated genotypes were separated electrophoretically, electro-transferred to nitrocellulose and probed with either α-mago polyclonal antibodies (upper panel) or α-myc monoclonal antibody 9E10 (below). Lane 1 contains ovarian protein extracts from the parental stock ($w^{1118}$) into which the p[*myc-mago*] construct was introduced and reveals a single, ~$17\times10^3$ $M_r$ protein detected by α-Mago antibodies. Lane 2 contains ovarian proteins from a strain containing two copies of p[*myc-mago*] (*myc*) on the X chromosome and two copies of wild-type *mago* on the second chromosome (+). Ovaries isolated from females homozygous for p[*myc-mago*] on the X chromosome and endogenous *mago* on the second chromosome, contain α-Mago immunoreactive proteins that migrate at ~$17\times10^3$ $M_r$ and ~$19\times10^3$ $M_r$. The myc-epitope adds ~$1.6\times10^3$ $M_r$ to the Mago protein, resulting in a detectable mobility shift in gel electrophoresis, relative to the $17.3\times10^3$ $M_r$ endogenous Mago protein. Lane 3 contains ovarian proteins from a strain containing two copies of p[*myc-mago*] on the X chromosome and no functional copies of *mago* on the second [*SHL-1*/*Df(2R)F36*]. An α-myc immunoreactive protein of ~$19\times10^3$ $M_r$ is detected only in the strains containing the p[*myc-mago*] transgene (lower panel).

We have used a monoclonal antibody recognizing the myc-epitope (Evan et al., 1985) to monitor the distribution of myc-Mago protein in oogenesis (for simplicity, we will refer to the myc-Mago protein as Mago protein throughout the remainder of the paper, except where it is essential to distinguish between myc-Mago and endogenous Mago protein). Ovaries from the parental strain $w^{1118}$ (not containing the p[*myc-mago*] transgene) reveal no staining above background when processed for immunofluorescence using the α-myc monoclonal antibody (Fig. 4H).

Whole-mount immunofluorescence on fixed ovarian tissue from p[*myc-mago*] strains using the α-myc monoclonal antibody reveals a striking pattern of Mago distribution during oogenesis. In the germarium, Mago is associated with all germ-line nuclei (data not shown). During stages 1 and 2, after the cyst leaves the germarium, Mago is detected within the nurse cell nuclei. By oogenetic stages 3-4, Mago is detected in the oocyte, both within the nucleoplasm and in the cytoplasm (Fig. 4A,B). Confocal microscopic analysis reveals that during the early stages of oogenesis (~1-7), the nurse cell nuclei contain Mago concentrated near the nuclear envelope (Fig. 4A-D) whereas the oocyte nucleus contains Mago throughout the nucleoplasm. As oogenesis continues Mago accumulates within the nurse cell nucleoplasm but is not detected within the prominent nucleoli (Fig. 4E). The distribution of myc-Mago and GFP-Mago throughout oogenesis are indistinguishable (compare Fig. 4E,G), providing evidence that these proteins accurately reflect the distribution of endogenous Mago. Within the oocyte nucleus, there is a region devoid of detectable Mago (Fig. 4A-D). Double-labelling with the DNA-binding stain DAPI reveals that this region is the karyosome, a region of condensed oocyte chromosomes (data not shown). Occasionally, a ‘spot’ containing Mago can be detected within the karyosome (Fig. 4A). This ‘spot’ may correspond to the endobody (originally, Binnenkörper in German), an ultrastructurally defined nuclear domain approximately 1 μm in diameter that is distinct from nucleoli (Bier et al., 1967; Mahowald and Tiefert, 1970).

Confocal microscopic analysis also reveals that Mago is associated with the posterior-most region of the oocyte. This posterior localization is observed during two distinct periods of oogenesis: the first during stages ~3-5, and the second during stages 8 and 9. During stages ~3-5, Mago is observed along the posterior periphery of the oocyte (Fig. 4A-C). At these stages, Mago is detected throughout the oocyte cytoplasm, with an apparent enrichment toward the posterior of the oocyte. During stages 6 and 7, Mago is not detected at the posterior pole, but remains associated with the germ-line nuclei (Fig. 4D). At stages 8 and 9, Mago is again detected at the posterior of the oocyte, at the site of pole plasm formation (Fig. 4E). By stage 10, Mago is no longer detectable at the posterior pole of the oocyte (data not shown).

Mago is also detected in the somatic follicle cell nuclei, but

is not detected within the nucleoli (Fig. 4E; King and Koch, 1963). Germ-line clonal analysis reveals that *mago*$^{+}$ function is required in the germ line (Table 1); thus, detection of Mago in somatic cells was somewhat unexpected. Egg chambers of strains containing p[*GFP-mago*] have detectable GFP-Mago within the nuclei of follicle cells. Furthermore, thirteen independent homozygous viable strains containing autosomal insertions of the p[*myc-mago*] transgene exhibit detectable myc-Mago in the nuclei of somatic follicle cells. Thus, the nuclear distribution of myc-Mago does not appear to be due to the presence of the myc epitope on the Mago protein nor does it appear that Mago localization within follicle nuclei is due to an enhancer element near the insertion site of the transgene.

The viable *mago* allele, *mago*$^{1}$ (GLY$^{19}$→ARG; Newmark and Boswell, 1994), when homo- or hemizygous disrupts the assembly of the posterior pole plasm during oogenesis. Given that wild-type Mago is localized within the posterior pole and required for the posterior pole localization of germ plasm (Newmark and Boswell, 1994), it was of interest to examine the distribution of Mago$^{1}$ protein within egg chambers. This was accomplished by introducing a myc-epitope into the 5′ coding sequences of a *mago* gene containing the *mago*$^{1}$ lesion (see Materials and Methods). The p[*myc-mago*$^{1}$] construct was introduced into the germ line by P-element-mediated transformation. Consistent with the *mago*$^{1}$ phenotype, p[*myc-mago*$^{1}$] complements the lethality of the zygotic lethal allele *SHL-1*, but the progeny of p[*myc-mago*$^{1}$] *SHL-1* homozygous females are sterile. Whole-mount immunolocalization on fixed ovarian tissues from p[*myc-mago*$^{1}$] strains reveals myc-Mago$^{1}$ within all germ-line nuclei and follicle nuclei of the egg chamber. In contrast to wild-type Mago, myc-Mago$^{1}$ is not detected within the posterior pole cytoplasm during oogenesis (Fig. 4F), demonstrating that posterior pole localization but not nuclear

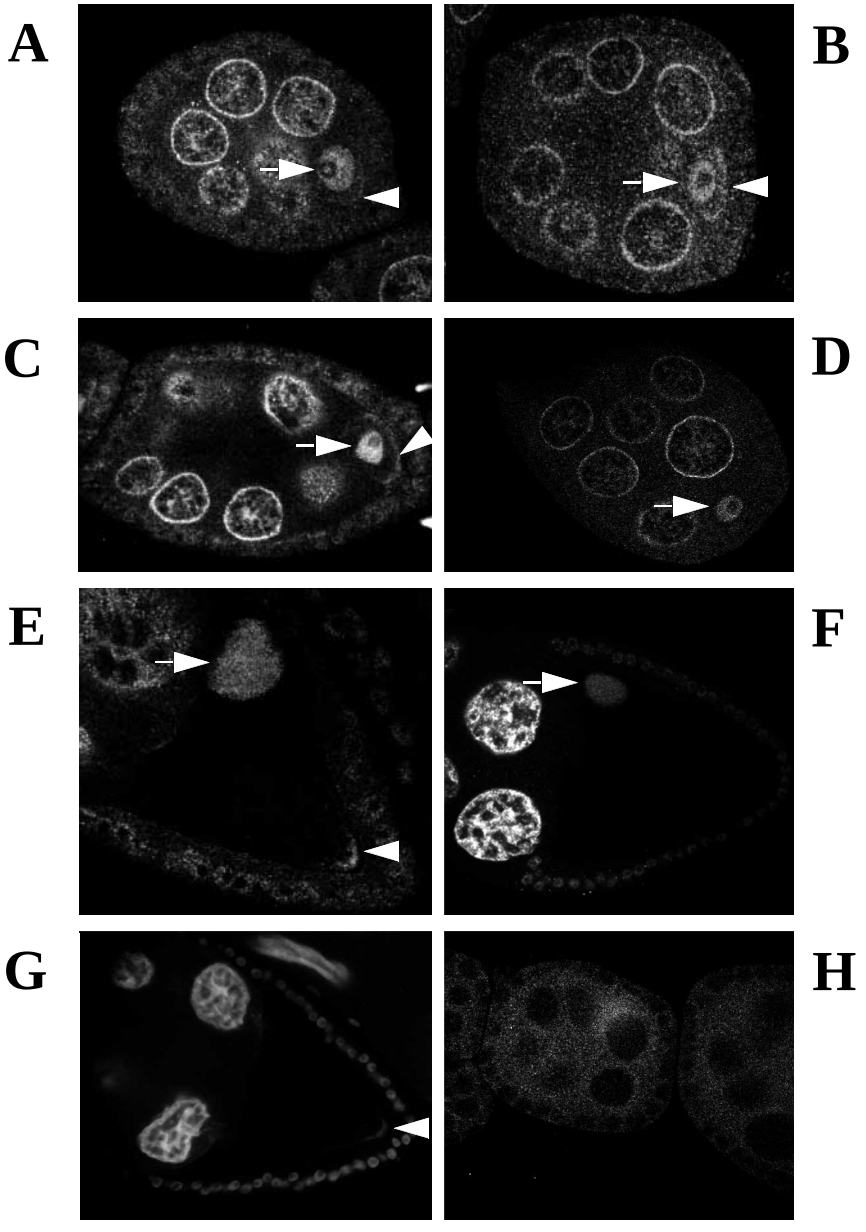


**Fig. 4**. myc-Mago, myc-Mago$^{1}$ and GFP-Mago localization during oogenesis. In all cases, the oocyte (at the posterior of the egg chamber) is oriented to the right. Arrows indicate the position of the oocyte nucleus and arrowheads the accumulation of Mago protein within the posterior pole of the oocyte. (A-E) Whole-mount immunolabeling using α-myc monoclonal 9E10 on egg chambers from females containing two X chromosomal copies of the p[*myc-mago*] transgene analyzed by confocal microscopy. (A) Egg chamber at approximately stage 3 of oogenesis. Note the accumulation of Mago throughout the oocyte nucleoplasm, as well as the 'spot' within the karyosome. Mago is also detected within the nurse cell nuclei. (B) Stage 4 egg chamber. Accumulation of Mago toward the posterior of the oocyte is observed. (C) Stage 5 egg chamber. A well-defined crescent of Mago is seen at the posterior of the oocyte. (D) At stages 6-7, Mago protein is not detectable at the oocyte posterior. (E) Localization of Mago within the oocyte posterior pole is again visible in a stage 9 egg chamber. Follicle cell nuclei also contain detectable Mago. (F) Whole-mount immunolabeling of a stage 9 egg chamber using α-myc monoclonal 9E10 on egg chambers from females containing two copies of the p[*myc-mago*$^{1}$] transgene and homozygous for *SHL-1*. myc-Mago$^{1}$ is detected in the follicle cell nuclei and germ-line nuclei but not in the posterior pole. (G) The distribution of Mago as revealed by two copies of the p[*GFP-mago*] transgene on the X chromosome. Mago protein is detected within the germ line in a pattern indistinguishable from wild type. (H) Egg chambers from *w*$^{1118}$ females (negative control) processed for immunolabelling using α-myc monoclonal 9E10. Only faint cytoplasmic background staining is detected.

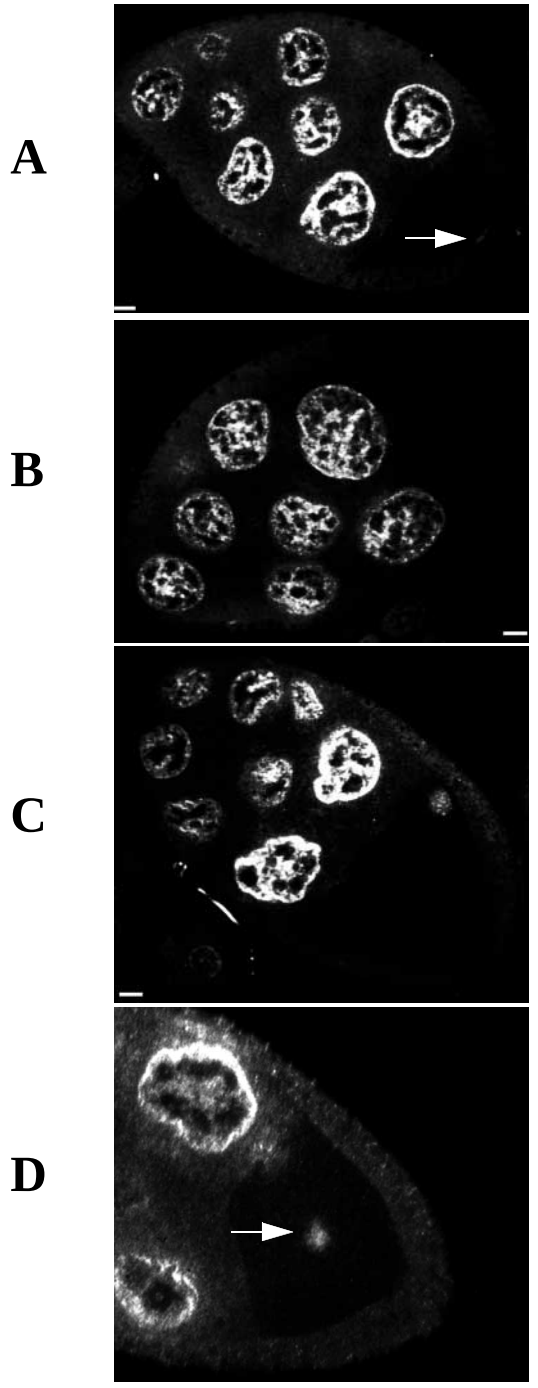


**Fig. 5**. Posterior Mago localization requires *cappuccino*$^{+}$, *spire*$^{+}$ and *gurken*$^{+}$ functions. (A-C) Egg chambers were obtained from females containing two X chromosomal copies of the p[*myc-mago*] transgene, as well as the second chromosome mutations indicated below. Posterior of the egg chamber is to the right. (A) Stage 8 egg chamber from a *vasa*$^{PD}$ homozygous female. The posterior localization of Mago (indicated by the arrow) is unaffected by this mutation. (B) Stage 8 egg chamber from *capu*$^{G7}$ homozygous female. Posterior Mago localization is not observed. (C) Stage 9 egg chamber from *spire*$^{RP48}$ homozygous female. Mago is not detected at the posterior pole. (D) Localization of Mago in egg chambers collected from females homozygous for *grk*$^{HK}$. myc-Mago is observed within a central region of the egg chamber (indicated by the arrow).

localization of Mago is critical for assembly of a functional posterior pole plasm.

### Posterior localization of Mago requires *cappuccino*$^{+}$, *spire*$^{+}$ and *gurken*$^{+}$ functions

Mutations in *cappuccino* (*capu*), *spire* (*spir*) and *grk* disrupt the posterior localization of the products of all previously identified posterior group genes (Manseau and Schüpbach, 1989; Ephrussi et al., 1991; Kim-Ha et al., 1991; St. Johnston et al., 1991; Bardsley et al., 1993; Wang et al., 1994; González-Reyes et al., 1995; Roth et al., 1995). Mutations in *capu* and *spir* result in premature commencement of microtubule-dependent cytoplasmic streaming during oogenesis (Theurkauf et al., 1992; Emmons et al., 1995); thus, they likely disrupt some cytoskeletal function required for posterior localization. Examination of Mago distribution in ovaries isolated from *capu* and *spir* homozygous females reveals that the posterior localization of Mago during stages 8-9 is disrupted (Fig. 5B, C). In contrast, the posterior localization of Mago protein in *vasa* homozygous mutant oocytes appears normal (Fig. 5A). Thus, gene products required early in the process of pole plasm assembly and localization (*capu* and *spir*) are required for posterior Mago localization, whereas one of the genes required later for pole plasm function (*vasa*) is not required for Mago localization. Mutations in *grk* disrupt the microtubule cytoskeleton and the egg chambers have germ-plasm components such as *osk* mRNA mislocalized to a central region of the cytoplasm (González-Reyes et al., 1995; Roth et al., 1995). In egg chambers from homozygous *grk*$^{HK}$ mothers, Mago is also localized in a central region of the oocyte cytoplasm (Fig. 5D), indicating that Mago colocalizes with germ-plasm components in *grk* mutants. These results are consistent with a role for Mago in the posterior localization of maternal determinants, rather than in the function of the determinants per se.

### *C. elegans mago* is a functional homologue of *Drosophila mago*

Homologues of *dm-mago* have been identified in *C. elegans* (*ce-mago*), *X. laevis* (*xl-mago*) and *M. musculus* (*mm-mago*). Database searches revealed a striking similarity between the *D. melanogaster mago* gene (*dm-mago*) and an expressed sequence tag isolated from early *C. elegans* embryos (Newmark and Boswell, 1994). The original cDNA, CEESH75, did not contain the entire coding sequence of *C. elegans mago* (*ce-mago*) and, therefore, was used to isolate near full-length *ce-mago* cDNAs. The predicted protein encoded by the largest *ce-mago* cDNA is 80% identical to *dm*-Mago (Fig. 6). If conservative substitutions are taken into account, it is 88% conserved (Fig. 6). Concomitantly, we screened *X. laevis* and *M. musculus* cDNA libraries (see Materials and methods) for full-length cDNAs. The predicted proteins encoded by *xl-mago* and *mm-mago* are 88% identical to *dm*-Mago (Fig. 6), indicating that Mago is highly conserved in these organisms.

Utilizing the most divergent homologue (*ce-mago*), we tested the hypothesis that the identified genes might be functional homologues of *dm-mago*. The coding sequence of *ce-mago* cDNA was cloned directly downstream of the promoter, 5′ untranslated region, and the first two codons of the *Drosophila mago* gene in a P-element transformation vector (see Materials and methods). This construct was then intro-

```
                10         20         30         40         50         60
              *    *     *    *     *    *     *    *     *    *     *    *
dm-mago       MSTEDFYLRY YVGHKGKFGH EFLEFEFRPD GKLRYANNSN YKNDTMIRKE AFVHQSVMEE
ce-mago       ekaa---v-- ---------- ---------n -s---g---- ---------- -t-se--ls-
xl-mago       -gs ------ ---------- ---------- ---------- ----v----- -y--k-----
mm-mago       -es ------ ---------- ---------- ---------- ----v----- -k--k-----

                70          80         90         100        110        120
dm-mago       LKRIIIDSEI MQEDDLPWPP PDRVGRQELE IVIGDEHISF TTSKTGSLVD VNRSKDPEGL
ce-mago       -----e---- -----dn--e --ki------ ---kn----- --g-i-a-a- --n----d--
xl-mago       -----d---v tk---al--- ---------- ---------- ----i---i- --q-------
mm-mago       -----d---- tk---al--- ---------- ---------- ----i---i- --q-------

                130       140
dm-mago       RCFYYLVQDL KCLVFSLIGL HFKIKPI
ce-mago       -s-------- ---------- -------
xl-mago       -v-------- ---------- -------
mm-mago       -v-------- ---------- -------
```

**Fig. 6**. Sequence alignment between proteins encoded by the *mago* genes from *D. melanogaster* (*dm*), *C. elegans* (*ce*), *X. laevis* (*xl*) and *M. musculus* (*mm*). Nonidentical residues in the *C. elegans*, *X. laevis* and *M. musculus* proteins are indicated as bold, lower case, letters. The dashes indicate identical residues and the two blanks at amino acid 4 represent residues not present in the *X. laevis* and *M. musculus* Mago proteins. The accession numbers for the sequences are AF007861 for *C. elegans mago* (*ce-mago*), AF007860 for *X.laevis mago* (*xl-mago*) and AF007862 for *M. musculus mago* (*mm-mago*).

duced into the *Drosophila* genome by P-element-mediated transformation (Rubin and Spradling, 1982). A single copy of *ce-mago* is sufficient to complement the axis defects and sterility of *mago*$^{1}$ and the zygotic lethality of the mutant *WE7* [both are point mutations in the *mago* gene (Newmark and Boswell, 1994)]. In contrast, two copies of *ce-mago* are necessary to complement the lethality of *SHL-1*, *mago*$^{3}$ and *RE7* [deletion and two nonsense mutations, respectively (Newmark and Boswell, 1994)]. Whether this dosage-dependent complementation is due to a lower abundance of *ce*-Mago protein or reduced function of *ce*-Mago protein relative to *dm*-Mago protein is unclear. Our α-*dm*-Mago antibodies do not recognize *ce*-Mago protein (data not shown), so we are unable to address this question at the present time. In either case, these results clearly indicate that *ce-mago* is able to provide *mago*$^{+}$ function(s) required for both germ-plasm assembly and zygotic viability; thus, *ce-mago* is a functional homologue of *dm-mago*.

## DISCUSSION

Mislocalization of the nucleus within the posterior pole of *mago* egg chambers suggests that *mago*$^{+}$ function is necessary to establish the spatial coordinates of the egg chamber. In ~36% of the stage 10 egg chambers collected from females hemizygous for the temperature-sensitive allele *mago*$^{1}$, shifted from 25˚C to 17˚C, the oocyte nucleus remains in the posterior pole (Fig. 1D). A similar mislocalization of the oocyte nucleus within the posterior pole is also observed in egg chambers of females mutant for *grk*, *top*/*DER* and *cni* (González-Reyes et al., 1995; Roth et al., 1995), and is sufficient to explain the occurrence of ventralized *mago* egg shells. Thus, *mago nashi* participates in the bidirectional intercellular signaling between the posterior follicle cells and oocyte to establish spatial coordinates that induce axis formation (González-Reyes et al., 1995; Roth et al., 1995).

In the absence of *top*/*DER* signaling during oogenesis, the fate of the posterior follicle cells is not specified and these cells take on an anterior fate. The consequence is that, instead of an aeropyle (an egg shell structure formed by the posterior follicle cells), a micropyle (anterior sperm entry site) is formed at the posterior pole; enhancer-trap lines that normally mark only the anterior follicle cells express β-galactosidase in follicle cells at the posterior pole. In contrast, females mutant for *mago* produce egg shells with an aeropyle that is indistinguishable from wild type. Utilizing enhancer-trap lines that serve as markers, we have established that in *mago* egg chambers posterior follicle cells are not transformed into anterior follicle cells. Although the oocyte nucleus is mislocalized in *mago* egg chambers, *grk* RNA and protein are synthesized and accumulate in a perinuclear position between the oocyte nucleus and plasma membrane, regardless of oocyte nucleus position. These results, and those described in Newmark and Boswell (1994), demonstrate that altering *mago*$^{+}$ function does not have a general effect on RNA or protein accumulation and localization.

To test the ability of *grk* to signal follicle cells in *mago* egg chambers, we monitored the expression of the enhancer-trap line, RA5, that is expressed in response to *grk* signaling (Duffy, personal communication). In *mago* egg chambers, RA5 is expressed in the posterior follicle cells overlying the mislocalized oocyte nucleus. Thus, the presence of an aeropyle in *mago* egg shells, the failure to detect a transformation of posterior follicle cells into anterior follicle cells and the pattern of expression of RA5 in *mago* egg chambers suggest that *grk-top/DER* signaling occurs normally in *mago* egg chambers. These results suggest that the primary signal from the oocyte to the posterior follicle cells is not disrupted in the absence of wild-type *mago* function.

Our current working model is that *mago*$^{+}$ function is necessary within the oocyte to mediate the response to the secondary signal sent to the oocyte by the posterior follicle cells. This model is supported by the analysis of germ-line clones. Disruption of anteroposterior and dorsoventral axis formation and posterior pole plasm assembly is observed when *mago*$^{+}$ function is altered in the germ line. In the absence of *mago*$^{+}$ function, the oocyte nucleus fails to migrate to an anterodorsal position and posterior pole components fail to localize.

The posterior localization of Mago during stages 3-5 and stages 8-9 of oogenesis suggests that *mago*$^{+}$ functions in at least two developmental processes: establishment of anteroposterior/dorsoventral polarity of the egg chamber, and anchoring of components within the posterior pole critical for anteroposterior polarity and germ cell determination during

embryogenesis. Here we have presented evidence that *mago*$^+$ functions within the germ line to mediate *grk-top/DER*-induced signaling from the posterior follicle cells to regulate reorganization of the cytoskeletal network. This cytoskeletal reorganization is critical for establishment of dorsoventral polarity. Thus, the posterior localization of Mago during stages 3-5 of oogenesis is consistent with a role for *mago* in mediating the *grk-top/DER*-induced signal from the posterior follicle cells to establish the anteroposterior/dorsoventral axes. Posterior localization of Mago during stages 8 and 9 of oogenesis corresponds to the stages when *osk* mRNA and Staufen protein are first localized (Ephrussi et al., 1991; Kim-Ha et al., 1991; St. Johnston et al., 1991). Unlike *osk* mRNA and Staufen protein, however, Mago is not detected at the anterior pole of the oocyte during stages 8 and 9. In mutant *mago* egg chambers, *osk* mRNA and Staufen protein localize within the anterior pole during these stages but are not detected within the posterior pole plasm (Newmark and Boswell, 1994). Although wild-type Mago localizes within the posterior pole, Mago$^1$ is not detected in the posterior pole of the oocyte. Thus, *mago*$^+$ function is essential for axis formation and anchoring/localization of components within the posterior pole.

The apparent absence of Mago from the posterior pole during stages 6 and 7 may reflect the reorganization of the oocyte cytoskeleton that takes place at these stages (Theurkauf et al., 1992). During stages 2-6, most microtubules are concentrated at the posterior of the oocyte (Theurkauf et al., 1992). By stage 7, the microtubules have reorganized so that they are concentrated at the anterior pole and an anterior-posterior gradient of microtubules begins to form (Theurkauf et al., 1992). If Mago localization relies on the microtubule cytoskeleton [as the localization of *osk* mRNA and Staufen protein appears to (Clark et al., 1994)] then this reorganization may temporarily disrupt the posterior localization of Mago.

We have shown that homologues of *Drosophila mago* exist in *C. elegans*, *X. laevis* and *M. musculus*. The evidence provided here indicates that the least conserved of these homologues, *ce-mago*, can replace *dm-mago* function in axis formation and posterior pole plasm assembly. There is already substantial experimental and morphological evidence suggesting that the mechanisms of germ cell determination may be conserved among distantly related animal groups. In both *Drosophila* and *Xenopus*, ultraviolet irradiation disrupts germ cell formation and transplantation of non-irradiated germ plasm restores germ-plasm formation (Smith, 1966; Okada et al., 1974; Warn, 1975). Ultrastructural analysis has revealed the presence of electron-dense structures in the germ lines of organisms representative of many different phyla, including Nematoda, Annelida, Arthropoda and Chordata (Eddy, 1975). These structures, termed 'nuage' or germinal granules, resemble the polar granules observed in the *Drosophila* germ line. Similar to polar granules, nuage consist of a fibrous material, lack surrounding membranes and are often observed in association with mitochondria or the nuclear envelopes of germ cells. It has been proposed that these structures play similar roles in specifying the germ cell lineage of highly divergent organisms (Beams and Kessel, 1974; Eddy, 1975). Given the similarities between the germ-line granules observed in *Drosophila*, *C. elegans* and *X. laevis*, as well as their germ-plasm localization and segregation into the germ cells during early embryogenesis, there has been speculation that these species may use similar mechanisms to construct their germ plasms. By demonstrating that *ce-mago* can functionally replace the *dm-mago* gene, we provide strong evidence that this speculation may be correct.

Localization of RNAs and/or proteins is critical for the establishment of polarity and germ cell determination in both invertebrates and vertebrates (Gurdon, 1992; St. Johnston and Nüsslein-Volhard, 1992). Asymmetrically distributed proteins have also been shown to act as cell fate determinants during neurogenesis (Lin and Schagat, 1997). In addition, reorganization of cytoskeletal components has been demonstrated to be important for establishment of axial polarity and specification of cell fate during neurogenesis (Gurdon, 1992; Guo and Kemphues, 1996; Lin and Schagat, 1997). Hence, a functional analysis of *mago* genes in *C. elegans*, *X. laevis* and *M. musculus* will indicate whether Mago is required for cytoskeletal reorganizations and RNA localization necessary to establish polarity, determine the germ line or specify somatic cell fates during development of these organisms.

We would like to thank: Clark Coffman, Joseph Duffy and Michael Klymkowsky for thoughtful comments on the manuscript; Robert Cary and Michael Klymkowsky for 9E10 monoclonal antibody and advice on confocal microscopy; Natasha Singh and Min Han for the *C. elegans* cDNA library; Barbara Knowles for the *Mus musculus* cDNA library; Joseph Duffy for the *grk* probe and the RA5 enhancer-trap line; Trudi Schüpbach for the *grk* and *top* alleles and the enhancer-trap lines 5A7 and BB127 and gurken antibody; Kathy Sotelo for the isolation of *mago* from *Xenopus*, Renee Walton for technical assistance, and Anne Bardsley, Clark Coffman, Joseph Duffy, Joe Heilig, and Jo Anne Powell-Coffman for helpful discussions. This work was supported by NIH training grant 2T32-GM07135 to P. A. N. and S. E. M., and NSF grant DCB 9119535 to R. E. B.; P. A. N. was the recipient of a Boettcher Foundation Pre-Doctoral Fellowship at the University of Colorado. R. E. B. is an Assistant Investigator of the Howard Hughes Medical Institute.

## REFERENCES

**Bardsley, A., McDonald, K. and Boswell, R. E.** (1993). Distribution of tudor protein in the *Drosophila* embryo suggests separation of functions based on site of localization. *Development* **119**, 207-219.

**Barstead, R. J. and Waterston, R. H.** (1989). The basal component of the nematode dense-body is vinculin. *J. Biol. Chem.* **264**, 10177-10185.

**Beams, H. W. and Kessel, R. G.** (1974). The problem of germ cell determinants. *Int. Rev. Cytol.* **39**, 413-479.

**Bier, K., Kunz, W. and Ribbert, D.** (1967). Struktur und funktion der oocytenchromosomen und nukleolen sowie der extra-DNS während der oogenese panoistischer und meroistischer insekten. *Chromosoma* **23**, 214-254.

**Boswell, R. E. and Mahowald, A. P.** (1985). *tudor*, a gene required for assembly of the germ plasm in *Drosophila melanogaster*. *Cell* **43**, 97-104.

**Boswell, R. E., Prout, M. E. and Steichen, J. C.** (1991). Mutations in a newly identified *Drosophila melanogaster* gene, *mago nashi*, disrupt germ cell formation and result in the formation of mirror-image symmetrical double abdomen embryos. *Development* **113**, 373-384.

**Chalfie, M., Tu, Y., Euskirchen, G., Ward, W. W. and Prasher, D. C.** (1994). Green fluorescent protein as a marker for gene expression. *Science* **263**, 802-805.

**Chou, T. B. and Perrimon, N.** (1996). The autosomal FLP-DFS technique for generating germline mosaics in *Drosophila melanogaster*. *Genetics* **144**, 1673-1679.

**Clark, I., Giniger, E., Ruohola-Baker, H., Jan, L. Y. and Jan, Y. N.** (1994). Transient posterior localization of kinesin fusion protein reflects anteroposterior polarity of the oocyte. *Curr. Biol.* **4**, 289-300.

**Eddy, E. M.** (1975). Germ plasm and differentiation of the germ line. *Int. Rev. Cytol.* **43**, 229-280.

**Emmons, S., Phan, H., Calley, J., Chen, W. L., James, B. and Manseau, L.** (1995). *cappuccino*, a *Drosophila* maternal effect gene required for polarity of the egg and embryo, is related to the vertebrate limb deformity locus. *Genes Dev.* **9**, 2482-2494.

**Ephrussi, A., Dickinson, L. K. and Lehmann, R.** (1991). *oskar* organizes the germ plasm and directs localization of the posterior determinant *nanos*. *Cell* **66**, 37-50.

**Ephrussi, A. and Lehmann, R.** (1992). Induction of germ cell formation by *oskar*. *Nature* **358**, 387-392.

**Evan, G. I., Lewis, G. K., Ramsay, G. and Bishop, J. M.** (1985). Isolation of monoclonal antibodies specific for human c-*myc* proto-oncogene product. *Mol. Cell. Biol.* **5**, 3610-3616.

**González-Reyes, A., Elliot, H. and St. Johnston, D.** (1995). Polarization of both major axes in *Drosophila* by *gurken-torpedo* signalling. *Nature* **375**, 654-658.

**Guo, S. and Kemphues, K. J.** (1996). Molecular genetics of asymmetric cleavage in the early *Caenorhabditis elegans* embryo. *Curr. Opin. Genet. Dev.* **6**, 406-415.

**Gurdon, J. B.** (1992). The generation of diversity and pattern in animal development. *Cell* **68**, 185-199.

**Kim-Ha, J., Smith, J. L. and Macdonald, P. M.** (1991). *oskar* messenger RNA is localized to the posterior pole of the *Drosophila* oocyte. *Cell* **66**, 23-34.

**King, R. C. and Koch, E. A.** (1963). Studies of the ovarian follicle cells of *Drosophila*. *Quart. J. Micr. Sci.* **104**, 279-320.

**Klingler, M. and Gergen, J. P.** (1993). Regulation of *runt* transcription by *Drosophila* segmentation genes. *Mech. Dev.* **43**, 3-19.

**Lane, M. E. and Kalderon, D.** (1994). RNA localization along the anteroposterior axis of the *Drosophila* oocyte requires PKA-mediated signal transduction to direct normal microtubule organization. *Genes Dev.* **8**, 2986-2995.

**Lehmann, R. and Nüsslein-Volhard, C.** (1986). Abdominal segmentation, pole cell formation, and embryonic polarity require the localized activity of *oskar*, a maternal gene in *Drosophila*. *Cell* **47**, 141-152.

**Lin, H. and Schagat, T.** (1997). Neuroblasts: a model for asymmetric division of stem cells. *Trends Genet.* **13**, 33-39.

**Lindsley, D. L. and Zimm, G. G. (**1992). *The Genome of Drosophila melanogaster*. San Diego: Academic Press, Inc.

**Mahowald, A. P. and Tiefert, M.** (1970). Fine structural changes in the *Drosophila* oocyte nucleus during a short period of RNA synthesis. *Wilhelm Roux' Arch. EntwMech. Org.* **165**, 8-25.

**Manseau, L. J. and Schüpbach, T.** (1989). *cappuccino* and *spire:* two unique maternal-effect loci required for both the anteroposterior and dorsoventral patterns of the *Drosophila* embryo. *Genes Dev.* **3**, 1437-1452.

**Newmark, P. A. and Boswell, R. E.** (1994). The *mago nashi* locus encodes an essential product required for germ plasm assembly in *Drosophila*. *Development* **120**, 1303-1313.

**Okada, M., Kleinman, I. A. and Schneiderman, H. A.** (1974). Restoration of fertility in sterilized *Drosophila* eggs by transplantation of polar cytoplasm. *Dev. Biol.* **37**, 43-54.

**Peifer, M., Orsulic, S., Sweeton, D. and Wieschaus, E.** (1993). A role for the *Drosophila* segment polarity gene *armadillo* in cell adhesion and cytoskeletal integrity during oogenesis. *Development* **118**, 1191-1207.

**Ray, R. P. and Schüpbach, T.** (1996). Intercellular signaling and the polarization of body axes during *Drosophila* oogenesis. *Genes Dev.* **10**, 1711-1723.

**Robertson, H. M., Preston, C. R., Phillis, R. W., Johnson-Schlitz, D. M., Benz, W. K. and Engels, W. R.** (1988). A stable genomic source of P element transposase in *Drosophila melanogaster*. *Genetics* **118**, 461-470.

**Roth, S., Neuman-Silberberg, F. S., Barcelo, G. and Schüpbach, T.** (1995). *cornichon* and the EGF receptor signaling process are necessary for both anterior-posterior and dorsal-ventral pattern formation in *Drosophila*. *Cell* **81**, 967-978.

**Rubin, G. M. and Spradling, A. C.** (1982). Genetic transformation of *Drosophila* with transposable element vectors. *Science* **218**, 348-353.

**Sambrook, J., Fritsch, E. F. and Maniatis, T.** (1989). *Molecular Cloning. A Laboratory Manual*. New York: Cold Spring Harbor Laboratory Press.

**Schüpbach, T. and Wieschaus, E.** (1986). Maternal-effect mutations altering the anterior-posterior pattern of the *Drosophila* embryo. *Roux's Arch. Dev. Biol.* **195**, 302-317.

**Shägger, H. and von Jagow, G.** (1987). Tricine-sodium dodecyl sulfate-polyacrylamide gel electrophoresis for the separation of proteins in the range from 1 to 100 kDa. *Anal. Biochem.* **166**, 368-379.

**Smith, L. D.** (1966). The role of a 'germinal plasm' in the formation of primordial germ cells in *Rana pipiens*. *Dev. Biol.* **14**, 330-347.

**St. Johnston, D.** (1993). Pole plasm and the posterior group genes. In *The Development of Drosophila melanogaster*, vol. I (ed. M. Bate and A. Martinez Arias), pp. 325-363. Plainview, NY: Cold Spring Harbor Laboratory Press.

**St. Johnston, D., Beuchle, D. and Nüsslein-Volhard, C.** (1991). *staufen*, a gene required to localize maternal RNAs in the *Drosophila* egg. *Cell* **66**, 51-63.

**St. Johnston, D. and Nüsslein-Volhard, C.** (1992). The origin of pattern and polarity in the *Drosophila* embryo. *Cell* **68**, 201-219.

**Theurkauf, W. E., Smiley, S., Wong, M. L. and Alberts, B. M.** (1992). Reorganization of the cytoskeleton during *Drosophila* oogenesis: implications for axis specification and intercellular transport. *Development* **115**, 923-936.

**Wang, C., Dickinson, L. K. and Lehmann, R.** (1994). Genetics of *nanos* localization in *Drosophila*. *Dev. Dynam.* **199**, 103-115.

**Wang, C. and Lehmann, R.** (1991). *nanos* is the localized posterior determinant in *Drosophila*. *Cell* **66**, 637-647.

**Warn, R.** (1975). Restoration of the capacity to form pole cells in u.v.-irradiated *Drosophila* embryos. *J. Embryol. Exp. Morph.* **33**, 1003-1011.

**Wieschaus, E. and Nüsslein-Volhard, C.** (1986). Looking at embryos. In *Drosophila: a Practical Approach*, vol. (ed. D. B. Roberts), pp. 199-227. Washington DC: IRL Press.

**Xue, F. Y. and Cooley, L.** (1993). *kelch* encodes a component of intercellular bridges in *Drosophila* egg chambers. *Cell* **72**, 681-693.

(Accepted 6 June 1997)